Table S1 List of exchanged variables in CAPS with the original coupling approach.

Variable	Source	Destination	Meaning
F_{swdn}	WRF	ROMS, CICE	Downward shortwave radiation at the surface
F_{lwdn}	WRF	ROMS, CICE	Downward longwave radiation at the surface
T_{2m}	WRF	ROMS, CICE	Air temperature at 2 m height
Q_{2m}	WRF	CICE	Specific humidity at 2 m height
RH	WRF	ROMS	Relative humidity at 2 m height
$\vec{U}_{10m}$	WRF	ROMS, CICE	Wind fields at 10 m height
$\vec{\tau}_{ao}$	WRF	ROMS	Wind stress at the atmosphere–ocean interface
$MSLP$	WRF	ROMS	Mean sea level pressure
P_{total}	WRF	ROMS, CICE	Total precipitation rate
E_{ao}	WRF	ROMS	Evaporation rate at the atmosphere–ocean interface
SST	ROMS	WRF, CICE	Sea surface temperature
SSS	ROMS	CICE	Sea surface salinity
W_{fr}	ROMS	CICE	Freezing/melting potential
$\vec{U}_o$	ROMS	CICE	Surface ocean currents
∇H_o	ROMS	CICE	Sea surface slope
A_{ice}	CICE	WRF	Sea ice concentration
T_{ice}	CICE	WRF	Ice surface temperature
α_{ice}	CICE	WRF	Surface albedo of snow and ice
$F_{swthru,io}$	CICE	ROMS	Penetrated shortwave radiation through sea ice
$F_{heat,io}$	CICE	ROMS	Net heat flux at the ice–ocean interface
$F_{water,io}$	CICE	ROMS	Freshwater flux at the ice–ocean interface
$F_{salt,io}$	CICE	ROMS	Salt flux at the ice–ocean interface
$\vec{\tau}_{io}$	CICE	ROMS	Ice–ocean stress

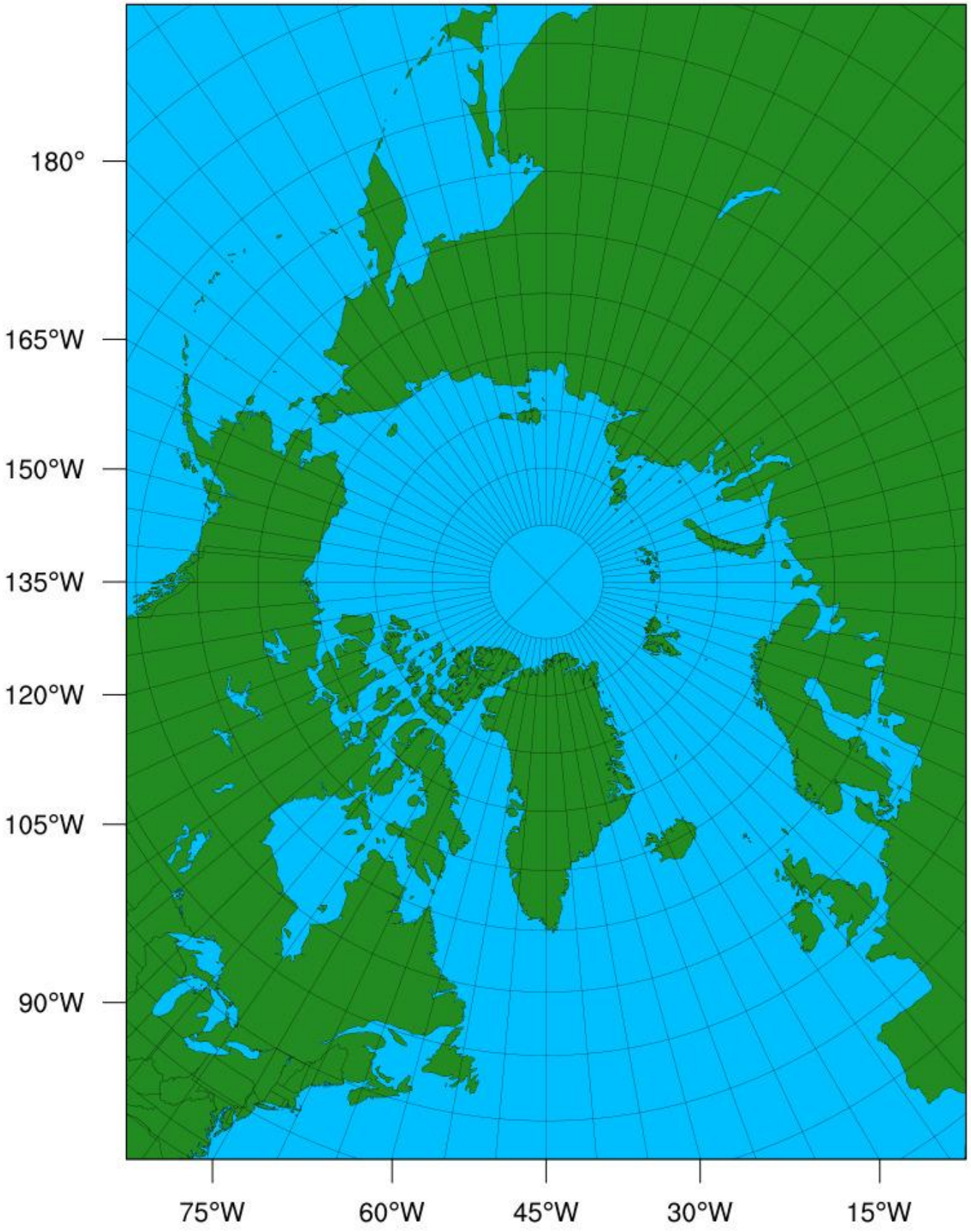

Figure S1 The model domain used in CAPS for pan-Arctic sea ice simulations.

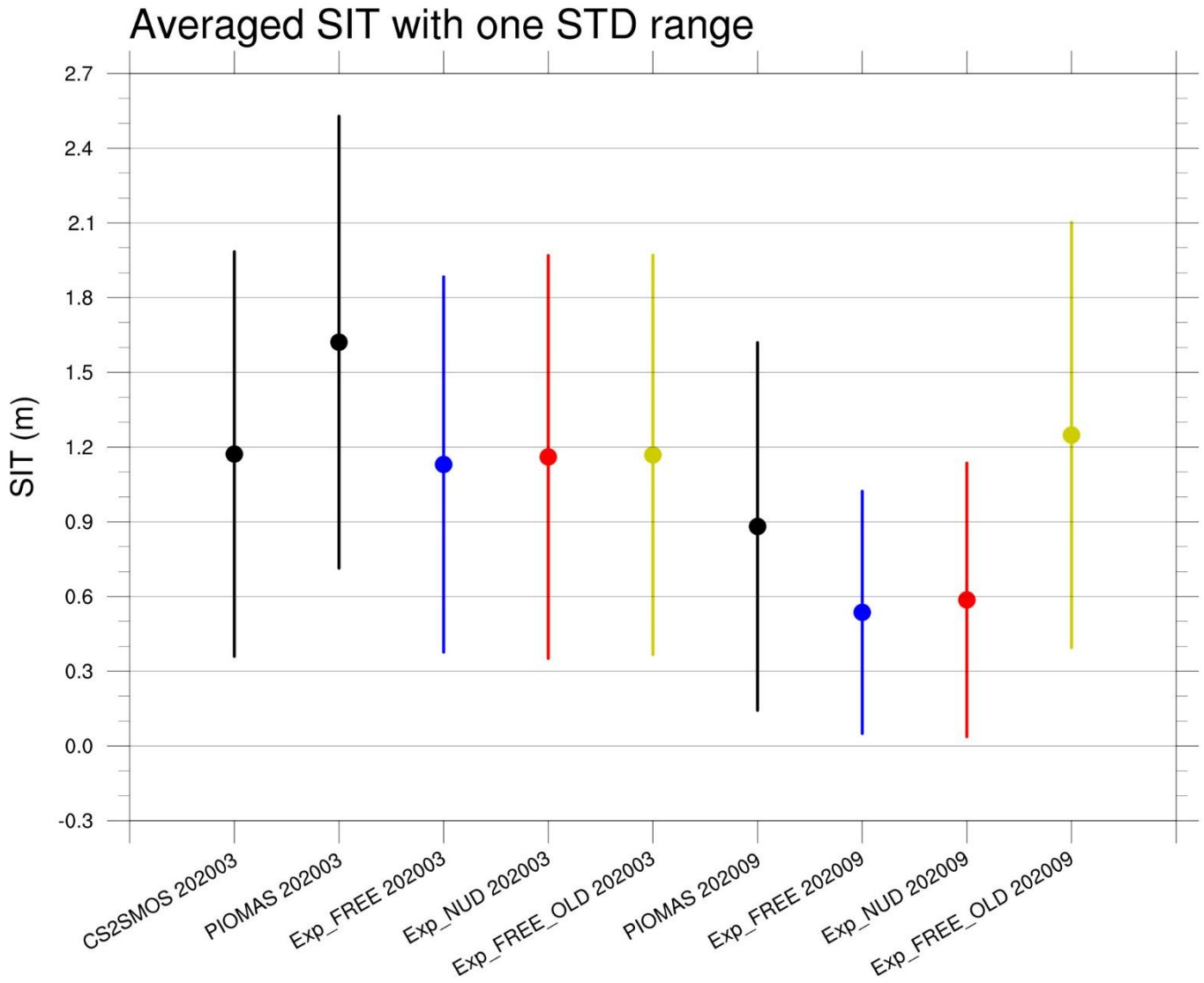

Figure S2 The average sea ice thickness of all cells with at least 1% sea ice concentrations for CS2SMOS, PIOMAS, Exp_FREE, Exp_NUD, and Exp_FREE_OLD in March and September 2020.

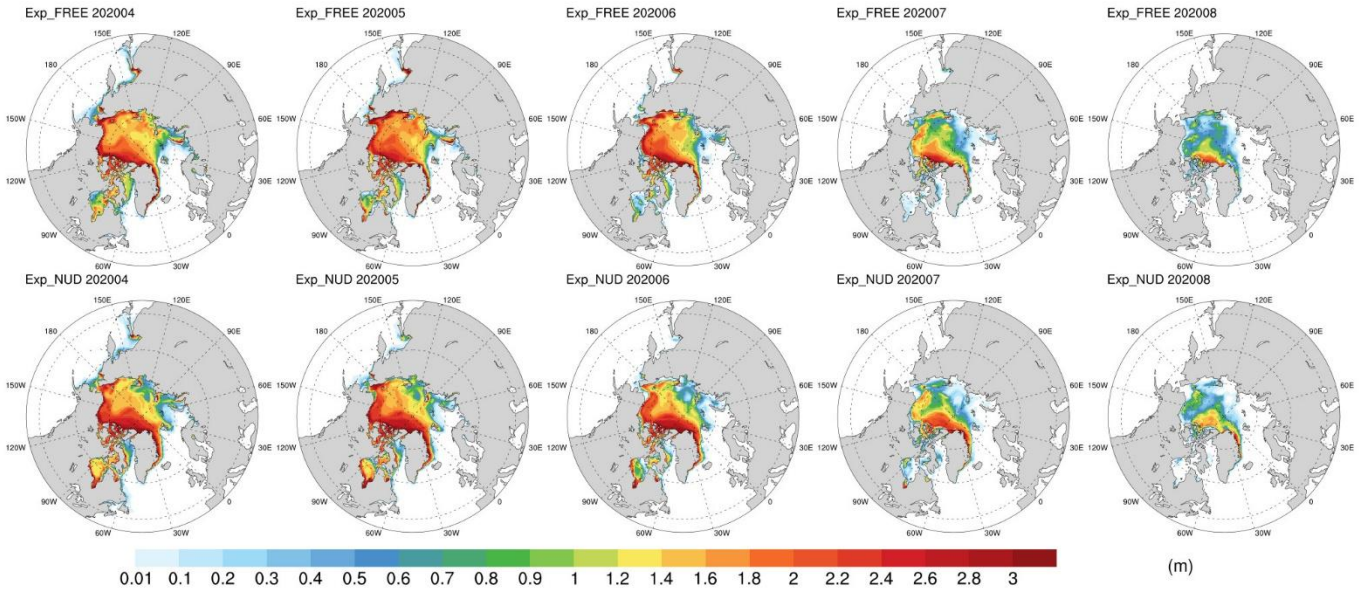

Figure S3 The monthly averaged sea ice thickness of Exp_FREE and Exp_NUD from April 2020 to August 2020.

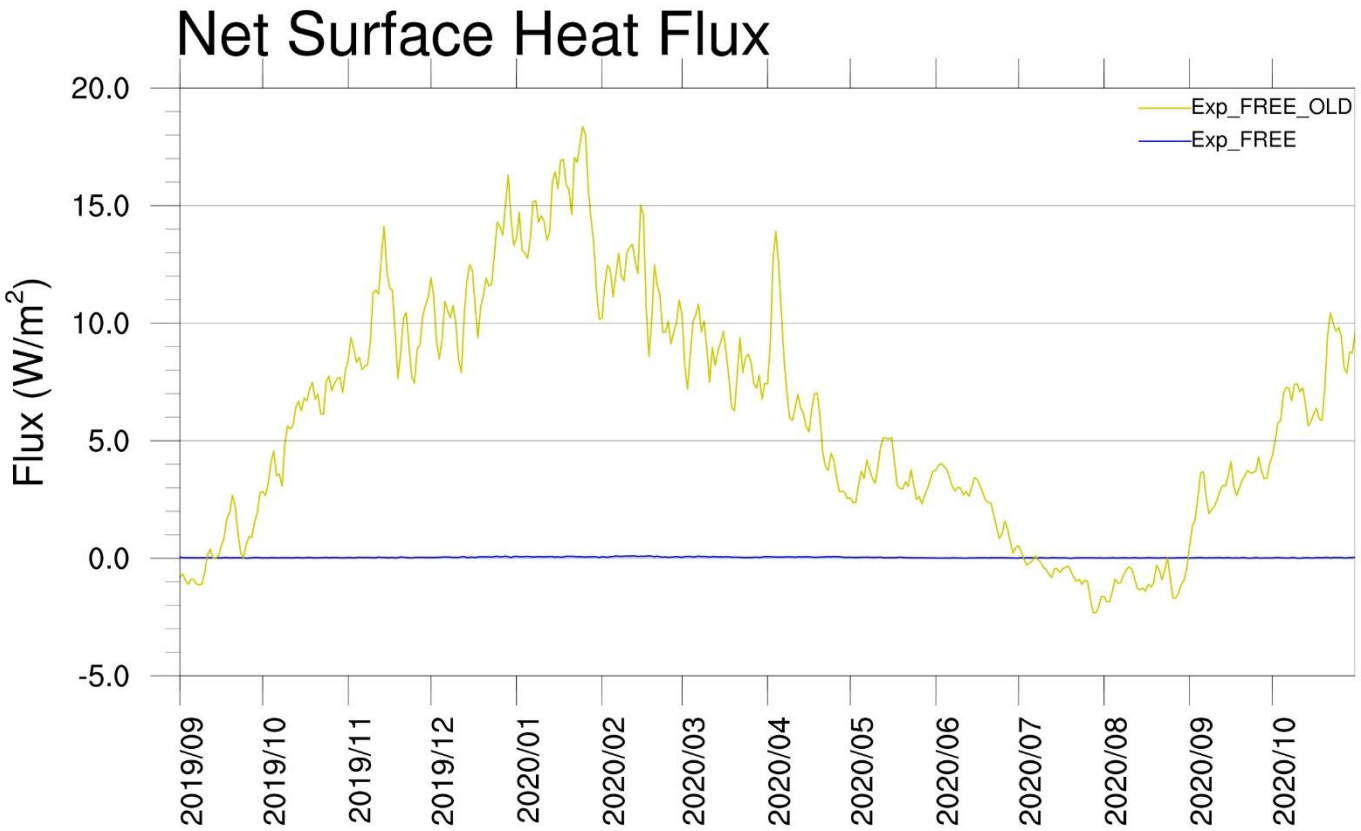

Figure S4 Same as Figure 6, but for differences between WRF and ROMS/CICE sides of net surface heat flux (combining net shortwave, net longwave, sensible, and latent heat fluxes).

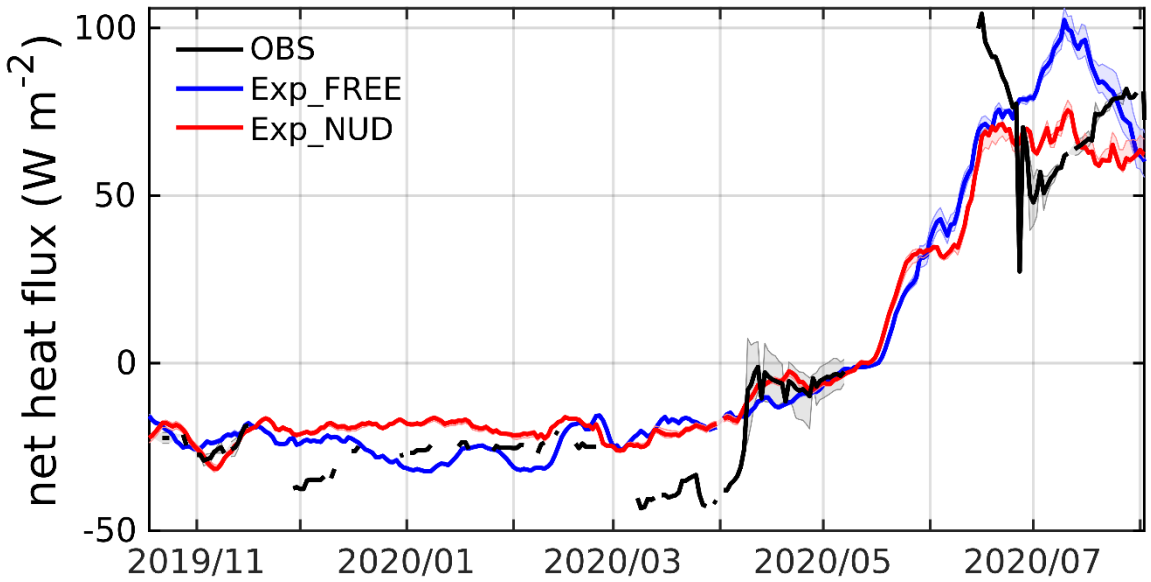

Figure S5 Same as Figure 11, but for net surface heat flux (combining net shortwave, net longwave, sensible, and latent heat fluxes).

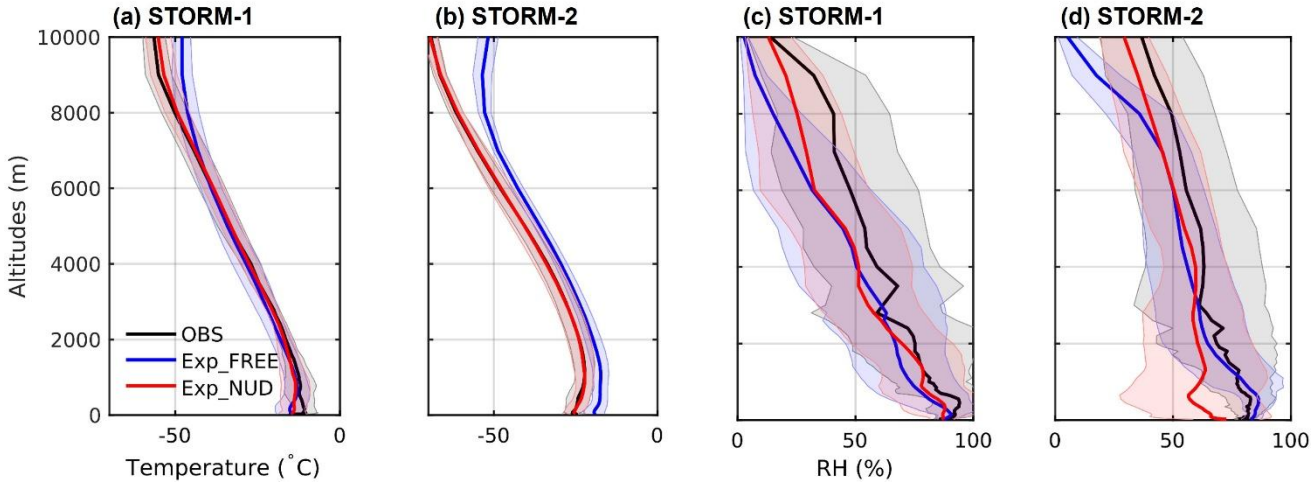

Figure S6 The averaged (a, b) temperature and (c, d) RH profiles for the observations (black line), Exp_FREE (blue line), and Exp_NUD (red line) during the STORM-1 period, and the STORM-2 period. Note: the shading represents one standard deviation range of corresponding variables.

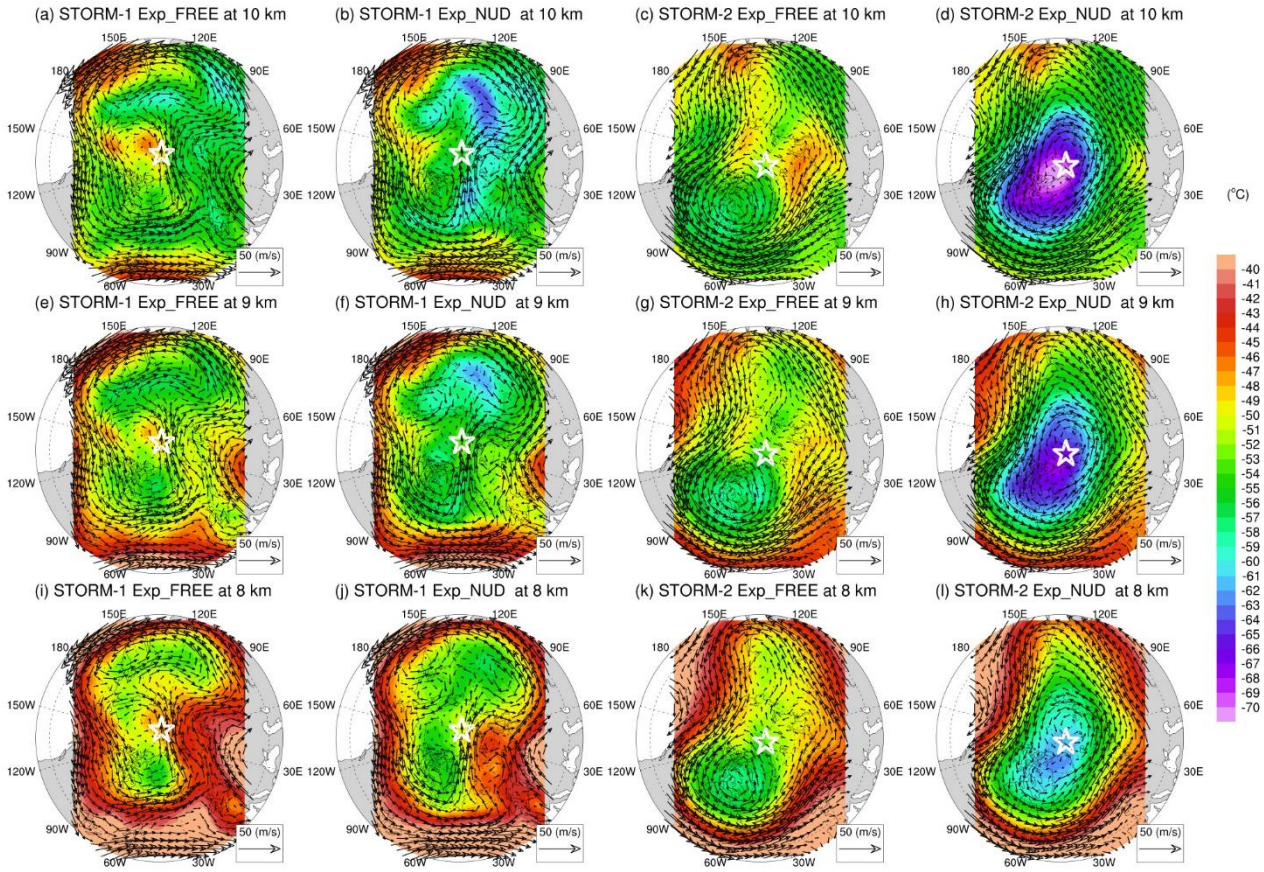

Figure S7 The averaged temperature and wind fields of (a, c, e, g, i, k) Exp_FREE, (b, d, f, h, j, l) Exp_NUD at 10, 9, and 8 km altitude during the STORM-1 and STORM-2 periods. Note: white star represents the averaged location of radiosondes during the STORM-1 and STORM-2 period.

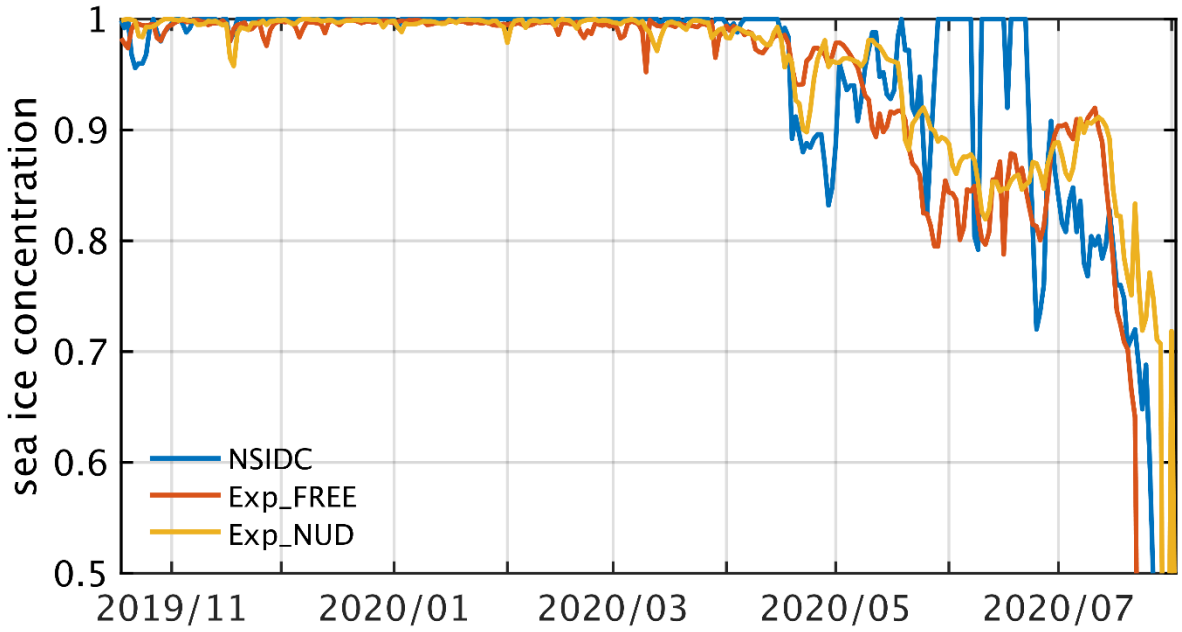

Figure S8 Time-series of sea ice concentration along the track of CTD buoys for the observations, Exp_FREE, and Exp_NUD.

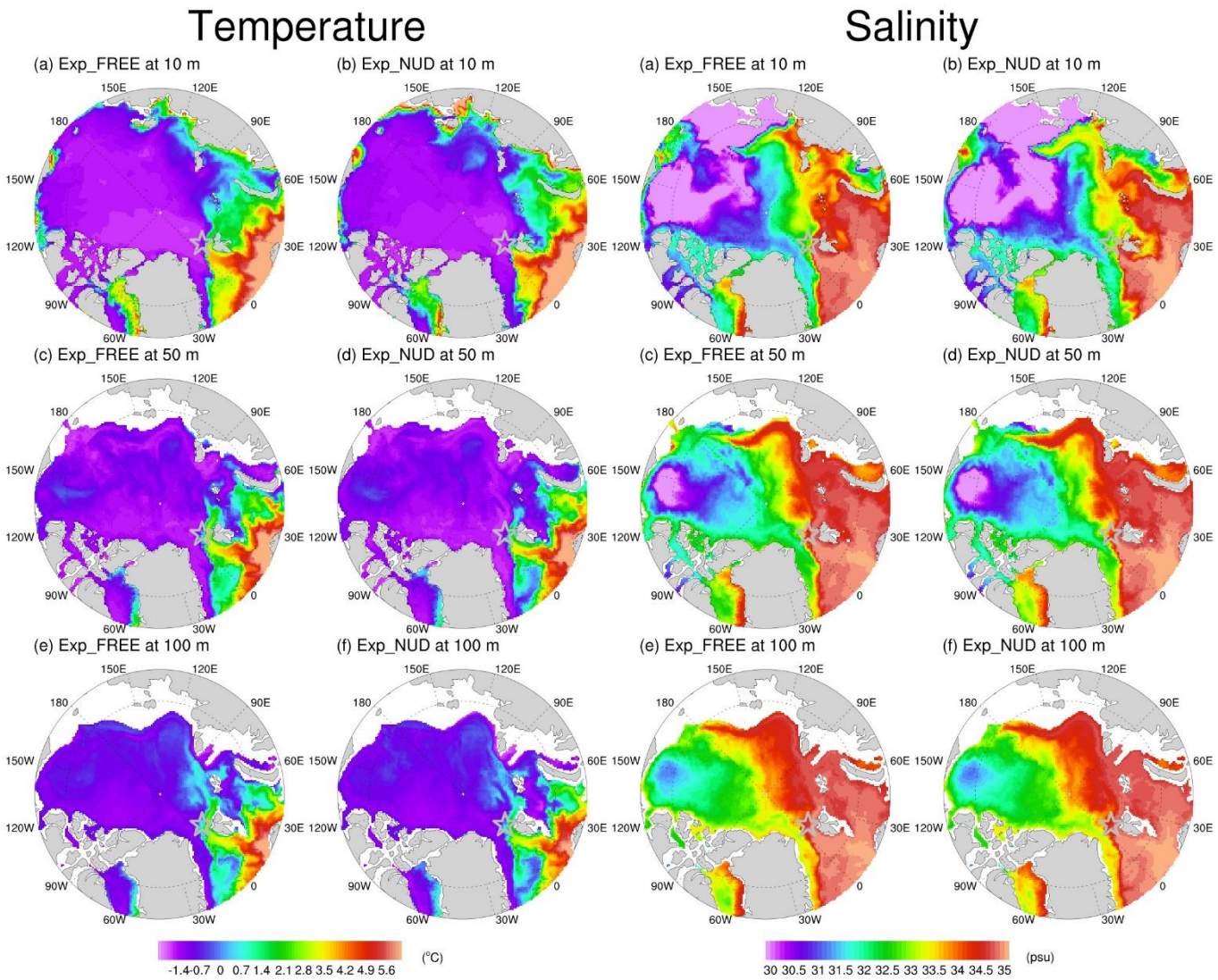

Figure S9 Daily-mean temperature (left panel) and salinity (right panel) of Exp_FREE and Exp_NUD at (a, b) 10, (c, d) 50, and (e, f) 100 m depth on July 1st, 2020. Note: gray star represents the averaged location of CTD buoys.

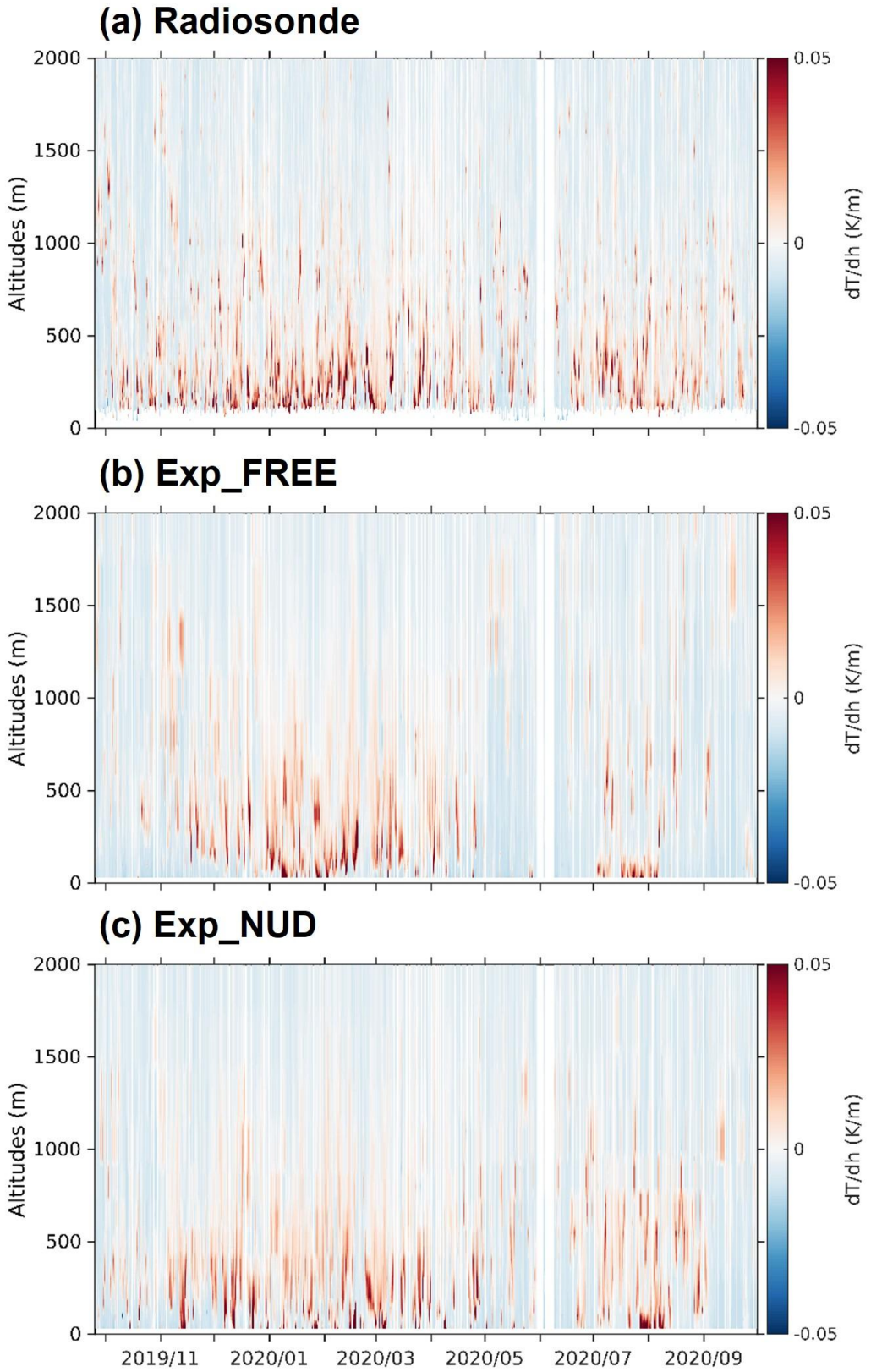

Figure S10 The evolutions of temperature lapse rate below 2 km altitude for (a) the radiosondes, (b) Exp_FREE, and (c) Exp_NUD along the track of MOSAiC drift.